An Extended Finite Element Method for Two-Phase Fluids

Jack Chessa* and Ted Belytschko†

March 5, 2002

Abstract

An extended finite element method with arbitrary interior discontinuous gradients is applied to two-phase immiscible flow problems. The discontinuity in the derivative of the velocity field is introduced by an enrichment with an extended basis whose gradient is discontinuous across the interface. Therefore, the finite element approximation can capture the discontinuities at the interface without requiring the mesh to conform to the interface, eliminating the need for remeshing. The equations for incompressible flow are solved by a fractional step method where the advection terms are stabilized by a characteristic Galerkin method. The phase interfaces are tracked by level set functions which are discretized by the same finite element mesh and are updated via a stabilized conservation law. The accuracy of the method is demonstrated in several examples.

KEYWORDS: enriched finite element, XFEM, level set, two-phase flow.

*Graduate Research Assistant, Northwestern University (j-chessa@northwestern.edu)

†Walter P. Murphy Professor of Mechanical Engineering, Northwestern University (t-belytschko@northwestern.edu)

1 Introduction

Two-phase flow problems are generally solved by two types of methods, interface-tracking algorithms or interface-capturing algorithms. Interface tracking methods use a deforming mesh or grid which conforms to the interface or tracks the interface in some other explicit manner. Examples are arbitrary Eulerian-Lagrangian (ALE) methods [15] and deforming space-time finite element formulations [34, 35]. In interface-capturing methods, an auxiliary function is defined on a fixed grid that describes the interface. Some examples of interface-capturing methods are volume of fluid methods (VOF) [19, 14], level set methods [20, 28] and marker and cell methods (MAC) [13].

The method described in this paper is an interface tracking method that shares many of the advantages of interface capturing methods: a fixed mesh is used, but we employ an enriched basis that includes the discontinuities at the interface. By embedding the interface jump conditions in the finite element basis, the accuracy of typical interface tracking methods is retained while remeshing is avoided. Remeshing can be quite expensive and can fail when the interface topology is significantly altered, as when phases join together or separate.

The methodology is called the extended finite element method (XFEM). The extended finite element method was first introduced by Belytschko and Black [2] and Moës *et al.* [18]. A general description of the method for modeling arbitrary discontinuities in a function and/or its derivatives is given by Belytschko *et al.* [4]. The idea for modeling discontinuities in derivatives used here originates from Krongauz and Belytschko [16], who developed it in the context of meshless methods. The extended finite element method was originally developed for crack problems but the methodology has been extended to several other problem classes. Sukumar *et al.* [29] introduced a combined level set and discontinuous XFEM to solve elastic problems involving holes and inclusions. Wagner *et al.* [37] solve problems involving particulate Stokes flow. Chessa *et al.* [6], Dolbow and Merle [10] and Renaud and Dolbow [25] applied XFEM to solidification problems.

We employ the level set method to track the interface, Osher and Sethian [20, 28]. The level set method is similar to pseudo-concentration methods [9, 36]; it describes the location of the interface by a signed scalar distance function, generally detonated as $\phi(\boldsymbol{x}, t)$ on the computational domain. The interface position is the set of points at which the level set field vanishes.

The extended finite element method couples naturally with the level set method. In the method proposed in this paper the enriched basis is constructed directly in terms of the level set $\phi(\boldsymbol{x}, t)$. Since $\phi(\boldsymbol{x}, t)$ is approximated by the same finite element mesh, the location of the discontinuity is expressed entirely in terms of nodal values of ϕ. Thus, as will be seen, the structure of the discontinuity and its approximation of the discontinuous field are expressed entirely in terms of nodal values of the velocity and level set function.

We extend the level set methods presented by Peng *et al.* [21] to finite element meshes to track the phase interface. The formulation by finite elements enhances the versatility of the method; it is applicable to problems that would be difficult to solve on a structured grid, *i.e.* problems that require local mesh refinement or problems involving complicated geometries and/or boundaries.

Finite element formulations of level set methods were first discussed by Barth and Sethian [1] with respect to triangulated domains. Since then several papers have used the level set method in a finite element context; Rao *et al.* [24], Chessa *et al.* [6] and Quecedo and Pastor [22]. However, level set methods are more commonly seen in finite difference schemes. This is probably due to the fact that finite difference methods are more widely used in solving the conservation law equations that are used to update the level set. Furthermore, some level set techniques rely on structured grids, *i.e.* fast marching methods. However, level set techniques are also very robust in finite element schemes. For example, Peng *et al.* [21] present an efficient PDE based method for updating the level set field in a region about the interface. They use finite difference schemes that are directly applicable to unstructured grids with no significant increase in cost or complexity.

The level set method has been used by Sussman *et al.* [30, 31, 32, 33] to solve two-phase incompressible flow problems with finite difference methods. Fedkiw *et al.* [5, 23] have used level sets in conjunction with ghost fluid methods to solve compressible-compressible and compressible-incompressible two-phase flows using finite difference schemes.

The outline of this paper is as follows; in Section 2 the governing equations are presented. In Section 3 we present the discontinuous finite element approximation for the velocity field. The finite element formulations for the level set update and the Navier-Stokes equations are presented in Sections 4 and 5 respectively. In Section 6 presents examples illustrating the accuracy and application of these methods.

2 Governing Equations

In this paper we consider isothermal incompressible two-phase flow which is described by the following equations for both phases

$$\rho\left(\frac{\partial \boldsymbol{u}}{\partial t} + \vec{\boldsymbol{\nabla}}\cdot(\boldsymbol{u}\otimes\boldsymbol{u}) - \boldsymbol{f}\right) - \vec{\boldsymbol{\nabla}}\cdot\boldsymbol{\sigma} = \mathbf{0} \tag{1}$$

$$\vec{\boldsymbol{\nabla}}\cdot\boldsymbol{u} = \mathbf{0} \tag{2}$$

where $\boldsymbol{u}$ is the velocity field, ρ is the fluid density, p is the hydrostatic pressure, $\boldsymbol{f}$ is an applied body force and $\boldsymbol{\sigma}$ is the Cauchy stress which is decomposed into the deviatoric stress $\boldsymbol{\tau}$, and the hydrostatic pressure as follows

$$\boldsymbol{\sigma} = \boldsymbol{\tau} - p\boldsymbol{I} \tag{3}$$

For a Newtonian fluid the deviatoric stress τ is given by

$$\boldsymbol{\tau} = 2\mu\boldsymbol{D} \tag{4}$$

with the rate of deformation tensor $\boldsymbol{D}$ defined as

$$\boldsymbol{D} = \frac{1}{2}\left(\vec{\boldsymbol{\nabla}}\boldsymbol{u} + \boldsymbol{u}\overleftarrow{\boldsymbol{\nabla}}\right) \tag{5}$$

Substituting (2-2) into (1), we obtain

$$\rho\left(\frac{\partial \boldsymbol{u}}{\partial t} + \vec{\boldsymbol{\nabla}}\cdot(\boldsymbol{u}\otimes\boldsymbol{u})\right) + \vec{\boldsymbol{\nabla}}p = \vec{\boldsymbol{\nabla}}\cdot(\mu\,\vec{\boldsymbol{\nabla}}\boldsymbol{u}) + \boldsymbol{f} \tag{6}$$

These equations hold over a domain Ω which is shown in Figure 1. The domain Ω is partitioned into Ω_1, $\Omega_2$where Ω_1 and Ω_2 are regions composed of fluids 1 and 2 respectively, and Γ_{int} is the interface between the two fluids. We assume that both phases are homogeneous and therefore the material properties are constant in Ω_1 and Ω_2 but since we solve (6) and (2) on Ω we consider ρ and μ to be functions of position and time due to the motion of the interface. The closure of Ω, $\partial\Omega$ is partitioned into Γ_u and Γ_T which are the boundaries where velocity and traction conditions are specified as follows

$$\boldsymbol{u}(\boldsymbol{x},t) = \bar{\boldsymbol{u}} \quad \forall\boldsymbol{x}\in\Gamma_u \tag{7}$$

$$\boldsymbol{n}\cdot\boldsymbol{\sigma}(\boldsymbol{x},t) = \bar{\boldsymbol{t}} \quad \forall\boldsymbol{x}\in\Gamma_t \tag{8}$$

We split the traction boundary condition into its normal and deviatoric components

$$p(\boldsymbol{x},t) = \bar{p} \quad \forall\boldsymbol{x}\in\Gamma_t \tag{9}$$

$$\boldsymbol{n}\cdot\boldsymbol{\tau}(\boldsymbol{x},t) = \bar{\boldsymbol{t}}_s \quad \forall\boldsymbol{x}\in\Gamma_t \tag{10}$$

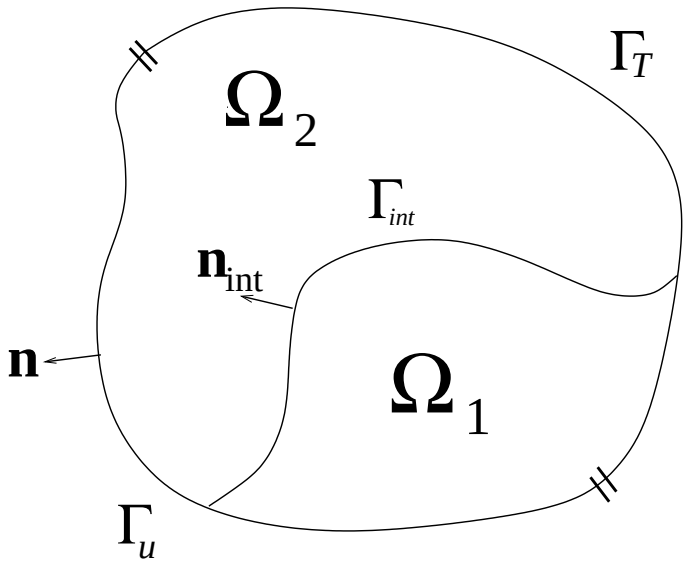


Figure 1: Problem domain

The vector $\boldsymbol{n}$ is an outward unit normal to Ω. Assuming negligible surface tension, no-slip and immiscible flow, the stress and velocity fields must satisfy the following conditions across the interface:

$$[\![\boldsymbol{n}_{int} \cdot \boldsymbol{\sigma}]\!] = 0 \tag{11}$$

$$[\![\boldsymbol{u}]\!] = 0 \tag{12}$$

Where $\boldsymbol{n}_{int}$ is an outward unit normal from Ω_1. To track the fluid interface we define a level set field $\phi(\boldsymbol{x}, t)$ on Ω such that it conforms to the following sign convention.

$$\phi(\boldsymbol{x}, t) \begin{cases} > 0 & \forall\, \boldsymbol{x} \in \Omega_1 \\ = 0 & \forall\, \boldsymbol{x} \in \Gamma_{int} \\ < 0 & \forall\, \boldsymbol{x} \in \Omega_2 \end{cases} \tag{13}$$

Using this convention we can define the material properties on the entire domain as a function of ϕ

$$\rho(\phi) = \begin{cases} \rho_1 & \phi \geq 0 \\ \rho_2 & \phi < 0 \end{cases} \quad \forall \boldsymbol{x} \in \Omega \tag{14}$$

$$\mu(\phi) = \begin{cases} \mu_1 & \phi \geq 0 \\ \mu_2 & \phi < 0 \end{cases} \quad \forall \boldsymbol{x} \in \Omega \tag{15}$$

or

$$\rho(\phi) = \rho_2 + \mathcal{H}(\phi)(\rho_1 - \rho_2) \quad \forall \boldsymbol{x} \in \Omega \tag{16}$$

$$\mu(\phi) = \mu_2 + \mathcal{H}(\phi)(\mu_1 - \mu_2) \quad \forall \boldsymbol{x} \in \Omega \tag{17}$$

where $\mathcal{H}(\cdot)$ is the Heaviside function. Furthermore, we define a signed distance function $d(\boldsymbol{x}, t)$ as

$$d(\boldsymbol{x}, t) = \min_{\bar{\boldsymbol{x}} \in \Gamma_{int}} \|\boldsymbol{x} - \bar{\boldsymbol{x}}\| sign(\boldsymbol{n}_{int} \cdot (\boldsymbol{x} - \bar{\boldsymbol{x}})) \tag{18}$$

and we require that initially

$$\phi(\boldsymbol{x}, t = 0) = d(\boldsymbol{x}, t = 0) \tag{19}$$

Since the fluids are immiscible we prohibit flow across the interface *i.e.*

$$\frac{\partial}{\partial t}\phi(\boldsymbol{X}, t) = 0 \quad \forall\, \boldsymbol{X} \in \Gamma_{int} \tag{20}$$

where $\boldsymbol{X}$ denotes the position of a point that remains on the interface. Expressing this condition in terms of spacial coordinates, we arrive at the standard level set evolution equation

$$\frac{\partial \phi}{\partial t} + \boldsymbol{u} \cdot \vec{\boldsymbol{\nabla}}\phi = 0 \tag{21}$$

This equation is used to update the level set and consequently update the interface location.

3 Enriched Finite Element with Interior Discontinuous Gradient

The domain of the problem, Ω is subdivided into elements Ω_e associated with a set of nodes $\boldsymbol{x}_I$, $I = 1$ to n. The interpolation function (shape function) associated with node I is denoted by $N_I(\boldsymbol{x})$ and the set of all nodes by $\mathcal{N}$. Recall that the support of $N_I(\boldsymbol{x})$, which is the area over which it is nonzero, is limited to the elements connected to the node I, *i.e.* the support is compact. The support of a typical node I is shown in Figure 2. Since we are dealing with a second order partial differential equations (6), we choose the shape functions to be piecewise continuously differentiable, *i.e.* $C^0(\Omega)$.

The extended finite element approximation is constructed in terms of the level set function defined by (19) and the shape functions N_I. In constructing the approximation, we distinguish the nodes whose support is intersected by the interface Γ_{int} from all others; this set of nodes is denoted by $\mathcal{N}_{enrich}$.

Figure 2 illustrates which nodes are enriched for a typical example. The enriched approximation is given by

$$\begin{aligned} \boldsymbol{u}^h(\boldsymbol{x},t) &= \sum_{I\in\mathcal{N}} N_I(\boldsymbol{x})\boldsymbol{U}_I(t) + \\ &\qquad \sum_{J\in\mathcal{N}_{enrich}} N_J(\boldsymbol{x})\Big(|\phi^h(\boldsymbol{x},t)| - |\phi^h(\boldsymbol{x}_J,t)|\Big)\boldsymbol{A}_J(t) \end{aligned} \tag{22}$$

where $\boldsymbol{U}_I(t)$ are the nodal parameters for the standard finite element approximation and $\boldsymbol{A}_J(t)$ are additional nodal parameters at the enriched node J. For convenience, we also write the above as

$$\boldsymbol{u}^h(\boldsymbol{x},t) = \sum_{I\in\mathcal{N}} N_I(\boldsymbol{x})\boldsymbol{U}_I(t) + \sum_{J\in\mathcal{N}_{enrich}} N_J^{enrich}(\boldsymbol{x},t)\boldsymbol{A}_J(t) \tag{23}$$

where

$$N_J^{enrich}(\boldsymbol{x},t) = N_J(\boldsymbol{x})\Psi_J(\boldsymbol{x},t) \tag{24}$$

$$\Psi_J(\boldsymbol{x},t) = |\phi^h(\boldsymbol{x},t)| - |\phi^h(\boldsymbol{x}_J,t)| \tag{25}$$

The second term in (25) is not essential but yields the desirable property that $\boldsymbol{u}^h(\boldsymbol{x}_I,t) = \boldsymbol{U}_I(t)$.

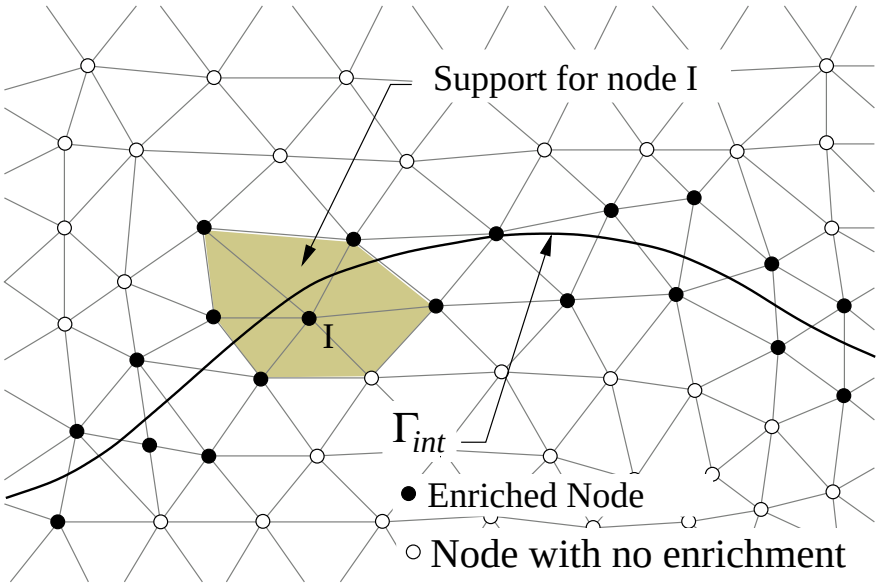


Figure 2: A typical finite element mesh with interface Γ_{int} showing the support of a generic node I and the enriched nodes

We next examine the character of this approximation around the interface Γ_{int}. Taking the gradient of (22) we obtain

$$\vec{\boldsymbol{\nabla}}\boldsymbol{u}^h = \sum_{I\in\mathcal{N}} \boldsymbol{U}_I(t)\otimes \vec{\boldsymbol{\nabla}}N_I + \sum_{J\in\mathcal{N}_{enrich}} \boldsymbol{A}_J(t)\otimes\Big(\vec{\boldsymbol{\nabla}}N_J\Psi_J + N_J\,\vec{\boldsymbol{\nabla}}\Psi_J\Big) \tag{26}$$

We next note that

$$\vec{\boldsymbol{\nabla}}\Psi_J = \text{sign}(\phi)\,\vec{\boldsymbol{\nabla}}\phi = \text{sign}(\phi)\boldsymbol{n}_{int} \tag{27}$$

where sign$(\cdot)$ is the sign of the number function and second equality follows from the fact that ϕ is distance function and therefore $|\,\vec{\boldsymbol{\nabla}}\phi| = 1$, see (18-19). Substituting (27) into (26) gives

$$\vec{\boldsymbol{\nabla}}\boldsymbol{u}^h = \sum_{I\in\mathcal{N}} \boldsymbol{U}_I(t)\otimes \vec{\boldsymbol{\nabla}}N_I + \sum_{J\in\mathcal{N}_{enrich}} \boldsymbol{A}_J(t)\otimes\Big(\vec{\boldsymbol{\nabla}}N_J\Psi_J + N_J\text{sign}(\phi)\boldsymbol{n}_{int}\Big) \tag{28}$$

Therefore the jump in $\boldsymbol{u}^h(\boldsymbol{x},t)$ across the interface is given by

$$[\![\vec{\boldsymbol{\nabla}}\boldsymbol{u}^h]\!] = 2\sum_{J\in\mathcal{N}_{enrich}} N_J\boldsymbol{A}_J\otimes\boldsymbol{n}_{int} \text{ on } \Gamma_{int} \tag{29}$$

and

$$[\![\vec{\boldsymbol{\nabla}}\boldsymbol{u}^h\cdot\boldsymbol{n}_{int}]\!] = 2\sum_{J\in\mathcal{N}_{enrich}} N_J\boldsymbol{A}_J \text{ on } \Gamma_{int} \tag{30}$$

The magnitude of the jump depends on $\boldsymbol{A}_I(t)$ and varies smoothly along the interface as can be seen from (30) since its spacial character results from the projection of the C^0 shape functions onto the interface. Note, that as with all piecewise continuous finite element approximations, $[\![\vec{\boldsymbol{\nabla}}\boldsymbol{u}]\!] \neq 0$ on the element edges, see [3].

The enrichment functions for a linear two-node element in one dimension are illustrated in Figure 3. Each enrichment function is a product of the shape function N_I, and the corresponding enrichment function $\Psi(\boldsymbol{x},t)$. Note that the enriched shape functions vanish at the nodes. The enrichment functions for a 3-node linear triangle are shown in Figure 4. As can be seen, each enrichment function vanishes along two of the edges. On the third edge a kink, similar to that what appears in the one-dimensional element, can be seen.

The character of this enrichment is of two types. The first type is within the elements cut by the interface; here all nodes are enriched and the enrichment is a partition of unity [17], so the enrichment function $\Psi(\boldsymbol{x},t)$ is reproduced

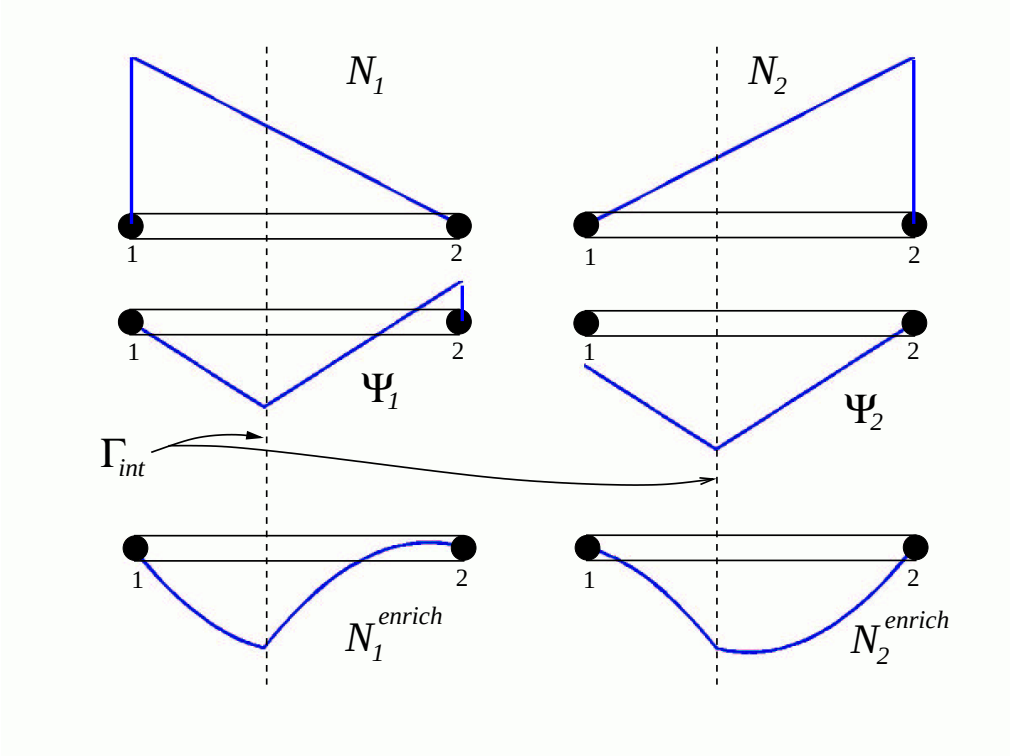


Figure 3: Example of an enriched finite element shape function in $\mathcal{R}^1$

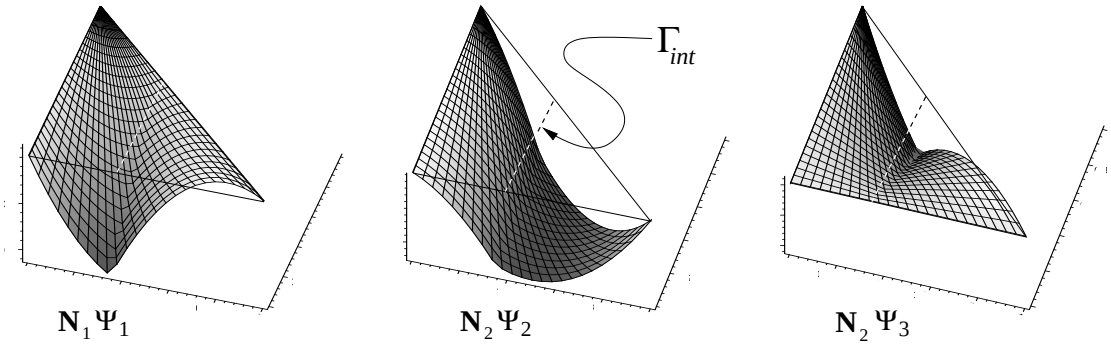


Figure 4: Enriched finite element shape function for a 3 node linear triangular element

exactly. The second type is within the elements adjacent to the fully enriched elements; here not all of the elements nodes are enriched. In these *partially* enriched elements the enrichment provides a *blending* so that the enrichment vanishes at the edge of the support of the bisected nodes. Figure 5 illustrates which elements are of the first and second types as well as those that are not enriched. The enrichment is local and the resulting system matrices are sparse.

The enrichment modifies the velocity field only in the elements crossed by the interface and in the adjacent elements that share the enriched nodes, see Figure 5. In other words, only the elements that lie entirely within the supports of shape functions cut by the interface are affected by the enrichment.

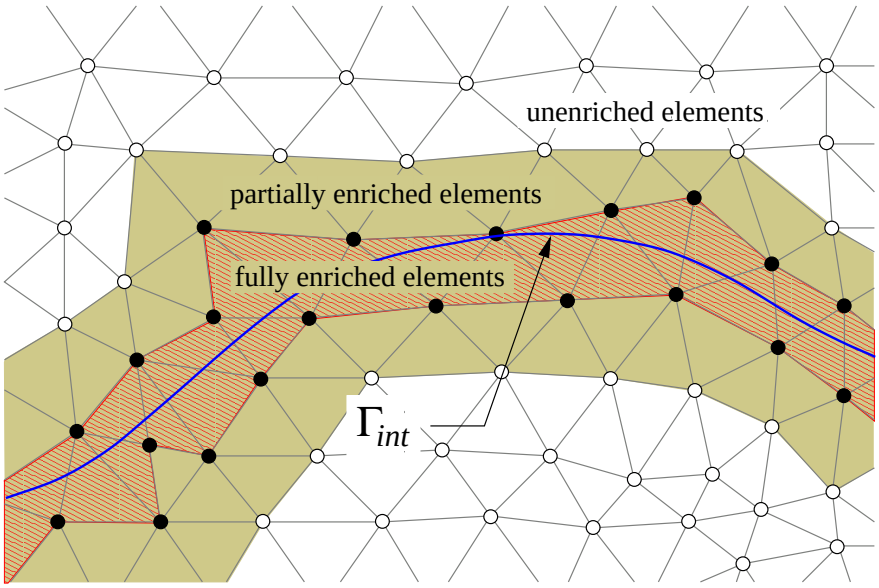


Figure 5: Enrichment for a typical finite element mesh, showing elements that are fully enriched, partially enriched and unenriched. Also illustrated is the boundary where the enrichment vanishes

The additional degrees of freedom $\boldsymbol{A}_J$ can be handled by adding nodes to the element or increasing the number of degrees of freedom for the enriched nodes. In either case, the modifications required in a standard finite element code are minimal.

4 Level Set Formulation

The level set function that tracks the interface is approximated by the same mesh and shape functions that are used for the velocity and pressure fields. However, no enrichment is needed for the level set function since it is continuously differentiable across the interface. Thus the level set approximation is given by

$$\phi^h(\boldsymbol{x},t) = \sum_{I\in\mathcal{N}} N_I(\boldsymbol{x})\phi_I(t) \tag{31}$$

where $\phi_I(t) = \phi(\boldsymbol{x}_I, t)$ are the nodal values of the level set. We follow the level set update method outlined in Peng *et al.* [21]. In this form Equation (21) is modified as follows

$$\frac{\partial\phi}{\partial t} + c(\phi)\,\boldsymbol{u}\cdot\vec{\boldsymbol{\nabla}}\phi = 0 \tag{32}$$

where $c(\phi)$ is a cut-off function that is defined by

$$c(\phi) = \begin{cases} 1 & \text{if } |\phi| \le \delta \\ (|\phi|-\gamma)^2(2|\phi|+\gamma-3\delta)/(\gamma-\delta) & \text{if } \delta < |\phi| \le \gamma \\ 0 & \text{if } |\phi| > \gamma \end{cases} \tag{33}$$

where δ is the cut-off distance from the interface and γ is transition distance. A characteristic method is used to stabilize the non self-adjoint term [39]. This, in conjunction with a forward Euler temporal discretization, yields the following update equation

$$\phi^{n+1} - \phi^n = -\Delta t\left[c(\phi)\boldsymbol{u}\cdot\vec{\boldsymbol{\nabla}}\phi - \frac{\Delta t}{2}\,\vec{\boldsymbol{\nabla}}\cdot\Big(c^2(\phi)(\boldsymbol{u}\otimes\boldsymbol{u})\cdot\vec{\boldsymbol{\nabla}}\phi\Big)\right]\Bigg|_{t=t^n} \tag{34}$$

where the superscript indicates the time step number and Δt is the time step. Using the standard Galerkin procedure *i.e.* the test and trial functions, $\phi^h(\boldsymbol{x},t)$ and $\psi^h(\boldsymbol{x})$ are in the same finite element function space $\mathcal{V}^h_\phi$, we get the following variational form of the update equation

$$\begin{aligned}\int_\Omega \psi(\phi^{n+1}-\phi^n)\,dV \;&=\; -\Delta t\int_\Omega \psi c(\phi)\boldsymbol{u}\cdot\vec{\boldsymbol{\nabla}}\phi\,dV \\ &\quad + \frac{\Delta t^2}{2}\int_\Omega \vec{\boldsymbol{\nabla}}\psi\cdot(c^2(\phi)\boldsymbol{u}\otimes\boldsymbol{u})\cdot\vec{\boldsymbol{\nabla}}\phi\,dV\end{aligned} \tag{35}$$

Because the hyperbolic nature of (21), a nonlinear viscous shock capturing operator $B_{sc}(\phi)$ is added, see Hansbo [12]. This minimizes the oscillations that may occur at discontinuities in curvature on the front. This operator is given by

$$B_{sc}(\phi) = \int_\Omega \nu_{sc}(\phi)(\,\vec{\boldsymbol{\nabla}}\psi\cdot\vec{\boldsymbol{\nabla}}\phi)\,dV \tag{36}$$

where ν_{sc} is a nonlinear viscosity defined as

$$\nu_{sc}(\phi) = h^e \sigma_{sc} \frac{|\frac{\partial \phi}{\partial t} + \boldsymbol{u} \cdot \vec{\boldsymbol{\nabla}} \phi|}{|\boldsymbol{u} \cdot \vec{\boldsymbol{\nabla}} \phi| + h^e} \tag{37}$$

σ_{sc} is a parameter used to control the degree of added viscosity (typically $\sigma_{sc} \approx 0.1$) and h^e is a measure of element e. The following variational formulation is used to update the level set field

$$\begin{aligned} \int_\Omega \psi(\phi^{n+1} - \phi^n)\, dV = -\Delta t \int_\Omega \psi c(\phi) \boldsymbol{u} \cdot \vec{\boldsymbol{\nabla}} \phi^n \, dV \\ + \frac{\Delta t^2}{2} \int_\Omega \vec{\boldsymbol{\nabla}} \psi \cdot (c^2(\phi) \boldsymbol{u} \otimes \boldsymbol{u}) \cdot \vec{\boldsymbol{\nabla}} \phi^n \, dV + \int_\Omega \nu_{sc} \, \vec{\boldsymbol{\nabla}} \psi \cdot \vec{\boldsymbol{\nabla}} \phi^n \, dV \end{aligned} \tag{38}$$

Because of the cut-off function, only the level set in the region $|\phi| \leq \delta$ needs to be updated in time. This significantly minimizes the computational overhead.

For some velocity fields ϕ may deviate significantly from a signed distance function after even a few time steps. This may cause high gradients in ϕ near the interface and introduce significant error in the interface position. These errors cause a loss of conservation of the phase volumes. This has often been cited as a shortcoming of the level set method and many interface-capturing methods [27, 26]. Extensional velocity fields and reinitialization are used to circumvent these difficulties [28, 8, 31, 32].

5 Navier-Stokes Formulation

We solve the Navier-Stokes equations by a characteristic based split (CBS) algorithm based on the projection method of Chorin [7] as described in Zienkiewicz and Codina [38] and Zienkiewicz and Taylor [39]. In this method an auxiliary velocity field $\boldsymbol{u}^*$ is introduced to uncouple the momentum and continuity equations; a characteristic method is used to stabilize the non self-adjoint operators in (6). The CBS formulation of (6) can be written as

$$\boldsymbol{u}^* - \boldsymbol{u}^n = \frac{\Delta t}{\rho}\Big[- \vec{\boldsymbol{\nabla}}\cdot(\rho \boldsymbol{u}\otimes\boldsymbol{u}) + \vec{\boldsymbol{\nabla}}\cdot\boldsymbol{\tau} - \rho\boldsymbol{f} + \frac{\Delta t}{2}(\boldsymbol{u}\cdot\vec{\boldsymbol{\nabla}})\Big(\vec{\boldsymbol{\nabla}}\cdot(\rho\boldsymbol{u}\otimes\boldsymbol{u}) + \rho\boldsymbol{f}\Big)\Big]\Big|_{t=t^n} \tag{39}$$

The final velocity field is *'corrected'* by the pressure increment so that is divergence free

$$\boldsymbol{u}^{n+1} - \boldsymbol{u}^* = \frac{\Delta t}{\rho}\,\vec{\boldsymbol{\nabla}} p^{n+1} \tag{40}$$

By taking the divergence of (40) and recalling that the velocity at time t^{n+1} must be divergence free (*i.e.* Equation 2) we arrive at the following Poisson equation for the pressure

$$\Delta t \nabla^2 p^{n+1} = \vec{\boldsymbol{\nabla}}\cdot(\rho\boldsymbol{u}^*) \tag{41}$$

Applying the standard Galerkin procedure on (39) for the fractional velocity field $\boldsymbol{u}^*$ we get the following

$$\int_\Omega \boldsymbol{W}\cdot(\boldsymbol{u}^* - \boldsymbol{u}^n)\,dV = \frac{\Delta t}{\rho}\Big[- \int_\Omega \boldsymbol{W}\cdot\vec{\boldsymbol{\nabla}}\cdot(\rho\boldsymbol{u}\otimes\boldsymbol{u})\,dV - \int_\Omega \Big(\vec{\boldsymbol{\nabla}}\boldsymbol{W}\Big) : \boldsymbol{\tau}\,dV + \int_{\Gamma_t} \boldsymbol{W}\cdot(\boldsymbol{n}\cdot\boldsymbol{\tau})\,dS - \int_\Omega \boldsymbol{W}\cdot(\rho\boldsymbol{f})\,dV - \frac{\Delta t}{2}\int_\Omega \Big(\vec{\boldsymbol{\nabla}}\cdot(\boldsymbol{u}\otimes\boldsymbol{W})\Big)\cdot\Big(\vec{\boldsymbol{\nabla}}\cdot(\rho\boldsymbol{u}\otimes\boldsymbol{u}) + \rho\boldsymbol{f}\Big)\,dV\Big]\Big|_{t=t^n} \tag{42}$$

where $\boldsymbol{W}$ is a test function. Similarly, the weak form for (41) is obtained by multiplying by the pressure test function V.

$$\int_\Omega \vec{\boldsymbol{\nabla}}V\cdot\vec{\boldsymbol{\nabla}}p^{n+1}\,dV = \frac{1}{\Delta t}\Big(\int_{\Gamma_u} V\,\vec{\boldsymbol{\nabla}}(p^{n+1} - p^n)\cdot\boldsymbol{n}\,dS - \int_\Omega \vec{\boldsymbol{\nabla}}V\cdot(\rho\boldsymbol{u}^*)\,dV - \int_{\Gamma_u} V(\rho\boldsymbol{u}^*)\cdot\boldsymbol{n}\,dS\Big) \tag{43}$$

To eliminate the boundary pressure terms we use (40) and require that $\boldsymbol{u}^* = \boldsymbol{u}$ on Γ_u yielding

$$\int_\Omega \vec{\boldsymbol{\nabla}}V\cdot\vec{\boldsymbol{\nabla}}p^{n+1}\,dV = \frac{1}{\Delta t}\Big(\int_\Omega \vec{\boldsymbol{\nabla}}V\cdot(\rho\boldsymbol{u}^*)\,dV - \int_{\Gamma_u} V(\rho\boldsymbol{u}^*)\cdot\boldsymbol{n}\,dS\Big) \tag{44}$$

and for the velocity correction equation (41)

$$\int_\Omega \boldsymbol{W}\cdot(\rho\boldsymbol{u}^{n+1})\,dV = \int_\Omega \boldsymbol{W}\cdot(\rho\boldsymbol{u}^*)\,dV + \Delta t\int_\Omega \boldsymbol{W}\cdot\vec{\boldsymbol{\nabla}}p^{n+1}\,dV \tag{45}$$

For the derivation of the finite element equations it is convenient to write the enriched approximation as

$$\boldsymbol{u}^h(\boldsymbol{x},t) = \bar{\mathbf{N}}(\boldsymbol{x},\phi)\bar{\mathbf{U}}(t) \tag{46}$$

where

$$\bar{\mathbf{N}}(\boldsymbol{x},\phi) = \left[\begin{array}{cccccccc} N_1, & N_2 & \ldots & N_n, & N_1\psi_1, & N_2\psi_2 & \ldots & N_{n_e}\psi_{n_e} \end{array}\right] \tag{47}$$

$$\bar{\mathbf{U}}(t) = \left[\begin{array}{cccccccc} \boldsymbol{U}_1, & \boldsymbol{U}_2 & \ldots & \boldsymbol{U}_n, & \boldsymbol{A}_1, & \boldsymbol{A}_2 & \ldots & \boldsymbol{A}_{n_e} \end{array}\right]^T \tag{48}$$

The finite element approximations are

$$\boldsymbol{W} = \bar{\mathbf{N}}^{n+1}\mathbf{W} \tag{49}$$

$$\boldsymbol{u}^n = \bar{\mathbf{N}}^n\bar{\mathbf{U}}^n \tag{50}$$

$$\boldsymbol{u}^* = \bar{\mathbf{N}}^{n+1}\bar{\mathbf{U}}^* \tag{51}$$

$$V = \mathbf{N}\mathbf{V} \tag{52}$$

$$p^n = \mathbf{N}\mathbf{p}^n \tag{53}$$

where the superscript n on $\bar{\mathbf{N}}^n$ indicates that enriched shape functions are a function of $\phi^n(\boldsymbol{x},t)$ (due to the moving enrichment). Substituting (50-53) into Equations (42-45) we obtain the following finite element equations

$$\mathbf{M}^*\bar{\mathbf{U}}^* = \mathbf{M}\bar{\mathbf{U}}^n - \Delta t\left[\mathbf{C}\bar{\mathbf{U}}^n + \mathbf{K}\bar{\mathbf{U}}^n - \mathbf{f}^n - \frac{\Delta t}{2}\left(\mathbf{K}_u\bar{\mathbf{U}}^n + \mathbf{f}_s^n\right)\right] \tag{54}$$

$$\Delta t\,\mathbf{K}_p\,\mathbf{p}^{n+1} = \mathbf{G}_u\bar{\mathbf{U}}^* - \mathbf{f}_p \tag{55}$$

$$\bar{\mathbf{U}}^{n+1} = \bar{\mathbf{U}}^* - \Delta t\mathbf{M}^{-1}\mathbf{G}^T\mathbf{p}^{n+1} \tag{56}$$

where

$$\mathbf{M}^* = \int_\Omega (\bar{\mathbf{N}}^{n+1})^T\rho^n\bar{\mathbf{N}}^n\,dV \tag{57}$$

$$\mathbf{M} = \int_\Omega (\bar{\mathbf{N}}^{n+1})^T\rho^n\bar{\mathbf{N}}^{n+1}\,dV \tag{58}$$

$$\mathbf{C} = \int_\Omega (\bar{\mathbf{N}}^{n+1})^T(\vec{\boldsymbol{\nabla}}(\rho^n\boldsymbol{u}^n\bar{\mathbf{N}}^n))\,dV \tag{59}$$

$$\mathbf{K} = \int_\Omega (\mathbf{B}^{n+1})^T\mu^n(\mathbf{I}_0 - \frac{2}{3}\mathbf{m}\mathbf{m}^T)\mathbf{B}^n\,dV \tag{60}$$

$$\mathbf{K}_u = -\frac{1}{2}\int_\Omega (\vec{\boldsymbol{\nabla}}^T(\boldsymbol{u}^n\bar{\mathbf{N}}^{n+1}))^T\rho^n(\vec{\boldsymbol{\nabla}}^T(\boldsymbol{u}^n\bar{\mathbf{N}}^n))\,dV \tag{61}$$

$$\mathbf{f} = \int_\Omega \bar{\mathbf{N}}^{n+1}\rho\boldsymbol{g}\,dV + \int_{\Gamma_t}\bar{\mathbf{N}}^{n+1}\boldsymbol{t}_s\,dS \tag{62}$$

$$\mathbf{K}_p = \int_\Omega (\vec{\boldsymbol{\nabla}}\mathbf{N})^T\,\vec{\boldsymbol{\nabla}}\mathbf{N}\,dV \tag{63}$$

$$\mathbf{G}_u = \int_\Omega (\vec{\boldsymbol{\nabla}}\bar{\mathbf{N}}^n)^T \rho^n \mathbf{N}^n \, dV \tag{64}$$

$$\mathbf{f}_p = \Delta t \int_{\Gamma_t} \mathbf{N}^T \boldsymbol{n} \cdot [\rho \boldsymbol{u}^n + \alpha \, (\rho \, \boldsymbol{u}^{n+1} - \rho \, \boldsymbol{u}^n - \Delta t \, \vec{\boldsymbol{\nabla}} p^{n+1})] \, dS \tag{65}$$

$$\mathbf{G} = \int_\Omega (\vec{\boldsymbol{\nabla}}\bar{\mathbf{N}}^{n+1})^T \bar{\mathbf{N}} \, dV \tag{66}$$

In the above $\mathbf{B}$ is the gradient matrix defined as

$$\mathbf{B}^n = \left[\begin{array}{cccc} \mathbf{B}_1^n & \mathbf{B}_2^n & \cdots & \mathbf{B}_n^n \end{array} \right]^T \tag{67}$$

$$\mathbf{B}_I^n = \left[\begin{array}{cc} \frac{\partial \bar{N}_I^n}{\partial x_1} & 0 \\ 0 & \frac{\partial \bar{N}_I^n}{\partial x_2} \\ \frac{\partial \bar{N}_I^n}{\partial x_2} & \frac{\partial \bar{N}_I^n}{\partial x_1} \end{array} \right] \tag{68}$$

$$\mathbf{I}_0 = \left[\begin{array}{ccc} 2 & & \\ & 2 & \\ & & 1 \end{array} \right] \tag{69}$$

$$\mathbf{m} = \left[\begin{array}{ccc} 1 & 1 & 0 \end{array} \right]^T \tag{70}$$

$$\tag{71}$$

It should be noted that when evaluating the gradient of the enriched shape functions $\bar{\mathbf{N}}$ the chain rule must be employed due to the spacial dependence of the level set field ϕ, so

$$\vec{\boldsymbol{\nabla}}\bar{N}_I = \vec{\boldsymbol{\nabla}} N_I \psi_I + N_I \, \vec{\boldsymbol{\nabla}} \psi_I \tag{72}$$

The update of the fluid/level set combination is as follows; given $\boldsymbol{u}^n$, p^n and ϕ^n we first explicitly update the level set as described in section 4 to obtain $\phi(\boldsymbol{x}, t^{n+1})$ then solve (54) for $\boldsymbol{u}^*$ then (55) for p^{n+1} and finally (5) for $\boldsymbol{u}^{n+1}$.

It should be noted that when evaluating these discontinuous finite element matrices and vectors that a quadrature rule must be used that will correctly integrate over elements where the discontinuity exists. Quadrature rules for these enriched methods are described in Chessa *et al.* [6] Moës *et al.* [18] and Sukumar *et al.* [29].

6 Example Problems

6.1 Interstitial fluid in a "Jogged" Channel

Consider the problem of a interstitial fluid flowing through a *"jogged"* channel as shown in Figure 6 at the initial time $t = 0$. The mesh is completely unstructured, as can be seen from Figure 6. An inlet velocity is prescribed at the left hand side, no slip boundary conditions are prescribed on the channel walls and a constant pressure condition is set on the right edge. The fluid is initially at rest and is slowly ramped up to a steady state value of 1.0. The steady state velocity field and interfaces are shown at several time

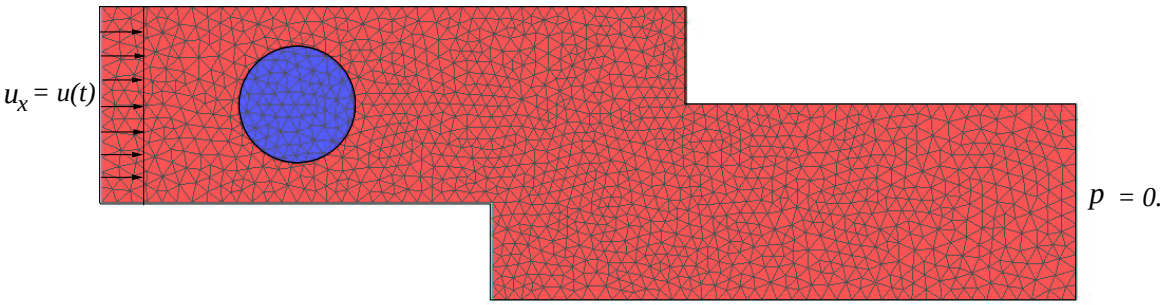


Figure 6: Initial configuration of interstitial fluid problem

steps in Figure 7. Note that the interface remains quite smooth, except for some kinking in the upper left hand corner in the final time step.

6.2 Bubble Rising to a Free Surface

Next we consider the problem of an immersed droplet of a secondary phase rising in a denser primary phase toward a free-surface as shown in Figure 8. Slip boundary conditions are given on the sides and the bottom edges and a constant pressure is prescribed at the top edge of the computational domain. The Reynolds number inside the bubble is 320 and for the surrounding fluid is 465. The results are qualitatively similar to the exact solution for a spherical droplet in an infinite media as given by Hadamard [11]. The interface is

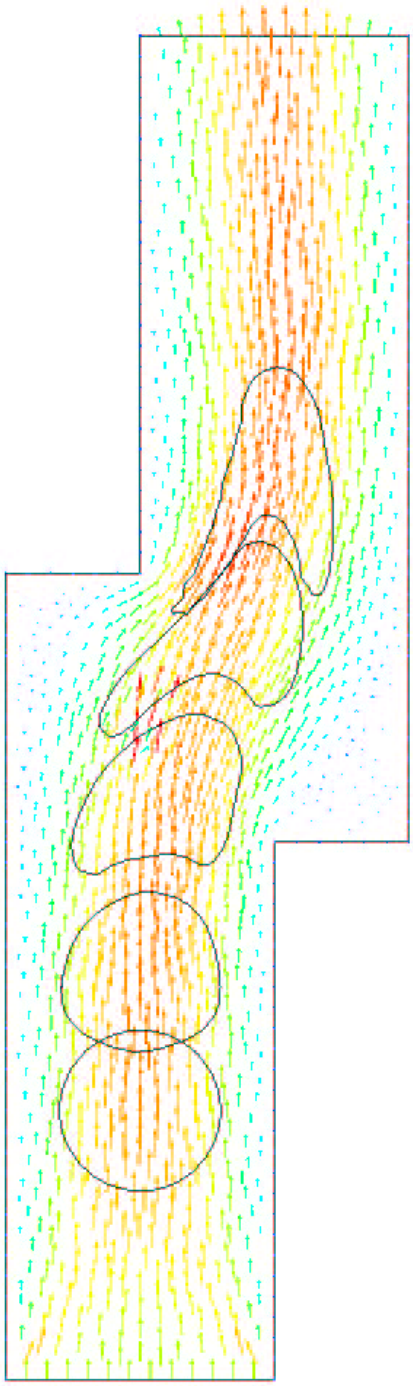


Figure 7: Phase interface at several time steps for interstitial fluid problem

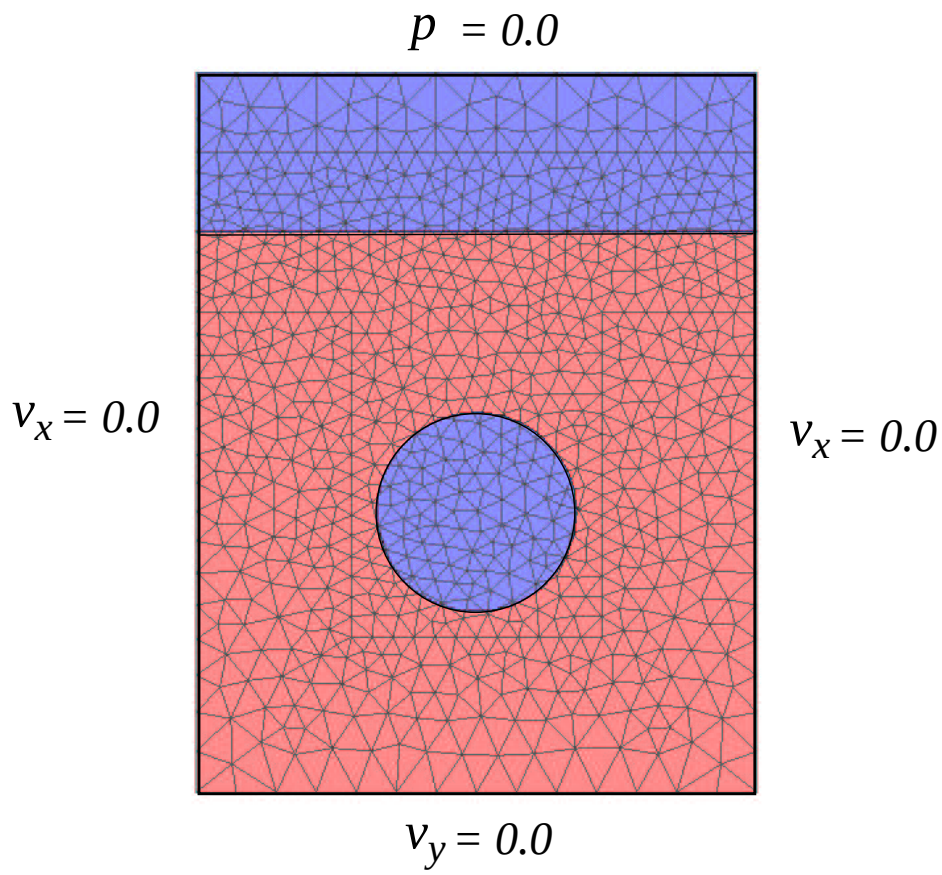


Figure 8: Rising bubble problem

shown for several time steps in Figure 9.

It should be noted that the level set method has no difficulty handling the large deformation of the interface and drastic topological changes associated with evolution of the bubble.

7 Conclusions

A method has been presented for modeling the evolution of discontinuous gradients in finite element methods. This method has been applied to two-phase flow problems in conjunction with the level set method to track phase interfaces. The method we employ to introduce the discontinuity in the gradient of the element basis thru a partition of unity. It can accurately resolve discontinuities in the velocity gradient at the interface without remeshing, even for materials with significantly differing viscosities. It is capable of handling highly deformed interfaces and interfaces where the topology significantly changes in a consistent and straight-forward manner.

The evolution of the interface in time is tracked by a level set method. A finite element formulation has been developed for the level set method. The finite element formulation allows the level set method to easily be applied to problems where mesh refinement is needed and problems with complex geometries and/or boundaries where a structured grid would be difficult. In contrast to methods such as VOF, the level set method has an explicit representation of the interface, and in contrast to methods involving indicator functions the level set method varies smoothly over the interface.

Both the strength of the discontinuity and its location are described by nodal values. The location is described by the nodal values of the level set ϕ_I, the strength of the discontinuity by the magnitude of the enrichment $\boldsymbol{A}_I$. This eliminates a need for geometric construction of the interface, so the extension to three dimensions can be readily accomplished.

8 Acknowledgments

The authors are grateful for the research support of the Office of Naval Research and the Department of Energy.

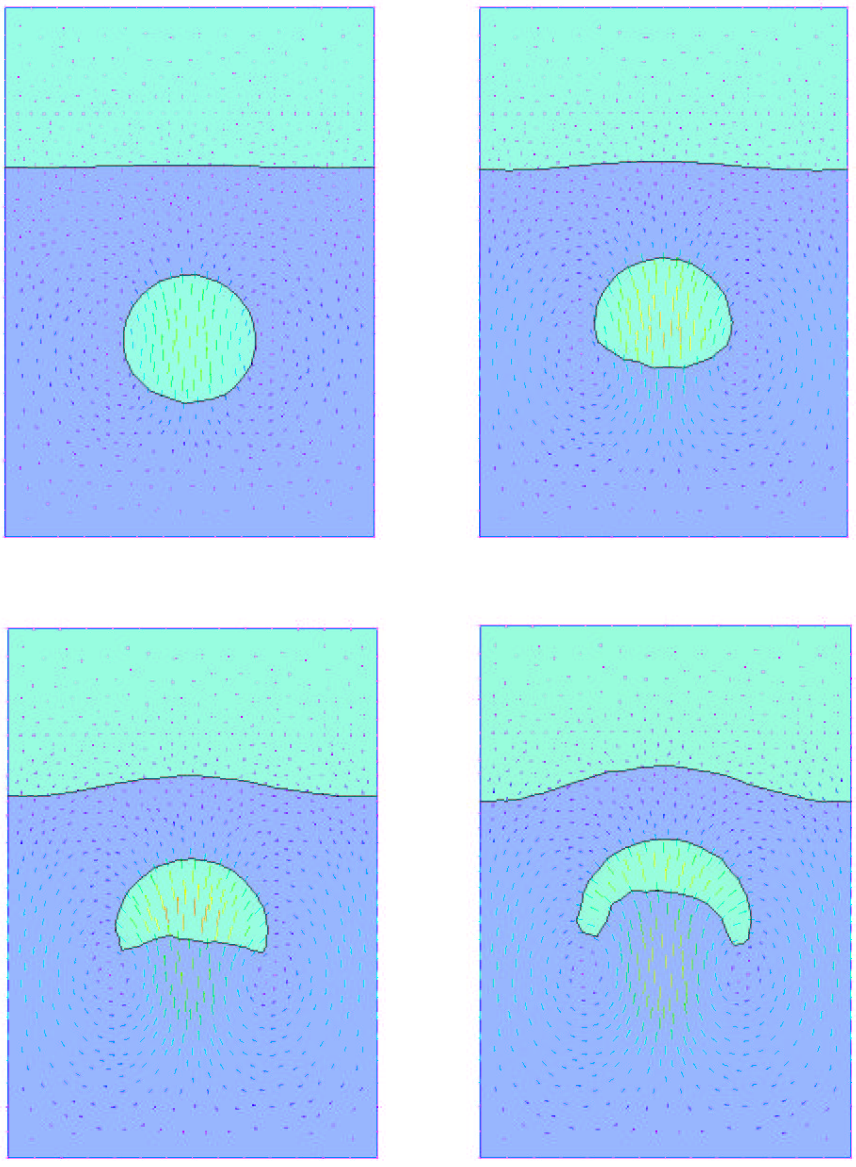


Figure 9: Phase interface for several time steps for rising bubble problem

References

[1] T. Barth and J. A. Sethian. Numerical schemes for the Hamilton-Jacobi and level set equations on triangulated domains. *Journal of Computational Physics*, 145:1–40, 1998.

[2] T. Belytschko and T. Black. Elastic crack growth in finite elements with minimal remeshing. *International Journal of Numerical Methods in Engineering*, 45(5):601–620, 1999.

[3] T. Belytschko, W.K. Liu, and B. Moran. *Nonlinear finite elements for continua and structures*. Wiley, 2000.

[4] T. Belytschko, N. Moës, S. Usui, and C. Parimi. Arbitrary discontinuities in finite element. *International Journal of Numerical Methods in Engineering*, 50(4):993–1013, 2001.

[5] R. Caide, R. P. Fedkiw, and C. Anderson. A numerical method for two-phase flow consisting of separate compressible and incompressible regions. *Journal of Computational Physics*, 166(1):1–27, 2001.

[6] J. Chessa, P. Smolinski, and T. Belytschko. The extended finite element method for Stefan problems. *International Journal of Numerical Methods in Engineering*, 2002. accepted for publication.

[7] A. J. Chorin. Numerical solution of the navier-stokes equation. *Math. Comput.*, 23:745–762, 1968.

[8] J. A. Sethian D. Adalstienson. The fast construction of extension velocities in level set methods. *Journal of Computational Physics*, 148:2–22, 1999.

[9] G. Dhatt, D.M. Gao, and A.B. Cheikh. A finite element simulation of metal flow in moulds. *International Journal of Numerical Methods in Engineering*, 30:821–831, 1990.

[10] J. Dolbow and R. Merle. Modeling dendritic solidification with the extended finite element method. In K.J. Bathe, editor, *Proceedings of the First MIT Conference on Computational Fluid and Solid Mechanics*, pages 1135–1138, Boston, 2001. Elsevier.

[11] J.S. Hadamard. *C .R. Acad. Sci.*, 152:1735, 1911.

[12] P. Hansbo. Explicit streamline diffusion finite element methods for the compressible Euler equations in conservation variables. *Journal of Computational Physics*, 109:274–288, 1993.

[13] J.H. Harlow and J.E. Welch. Numerical study of large amplitude free surface motion. *Physics of Fluids*, 9:842–851, 1966.

[14] C.W. Hirt and B.D. Nichols. Volume of fluid (VOF) method fo the dynamics of free boundaries. *Journal of Computational Physics*, 39(1):201–225, 1981.

[15] A. Huerta and W.K. Liu. Viscous flow with large free-surface motion. *Computer Methods in Applied Mechanics and Engineering*, 1988.

[16] Y. Krongauz and T. Belytschko. EFG approximation with discontinuous derivatives. *International Journal of Numerical Methods in Engineering*, 1997. accepted for publication.

[17] J.M. Melenk and I. Babuška. The partition of unity method: Basic theory and applications. *Computer Methods in Applied Mechanics and Engineering*, 139:289–314, 1996.

[18] N. Moës, J. Dolbow, and T. Belytschko. A finite element method for crack growth without remeshing. *International Journal of Numerical Methods in Engineering*, 46:131–150, 1999.

[19] W. Noh and P. Woodward. A simple line interface calculation. In A.I. vn de Vooran and P.J Zandberger, editors, *Proceedings, Fifth International COnference on Fluid Dynamics*. Springer-Verlag, 1976.

[20] S. Osher and J. A. Sethian. Propagation of fronts with curvature based speed: algorithms based on Hamilton-Jacobi formulations. *Journal of Computational Physics*, 79:12, 1988.

[21] D. Peng, B. Merriman, S. Osher, H. Zhao, and M. Kang. A PDE-based fast local level set method. *Journal of Computational Physics*, 155:410–438, 1999.

[22] M. Quecedo and M. Pastor. Application of the level set method to the finite element solution of two-phase flows. *International Journal of Numerical Methods in Engineering*, 50:645–663, 2001.

[23] T. B. Merriman R. P. Fedkiw, P. Aslam and S. Osher. A non-oscillatory eulerian approach to interfaces in multi-material flows. *Journal of Computational Physics*, to apear.

[24] V.S. Rao, T.J.R. Hughes, and K. Garikipati. On modeling thermal oxidation of silicon II: numerical aspects. *International Journal of Numerical Methods in Engineering*, 47:359–377, 2000.

[25] M. Renaud and J. Dolbow. Solving thermal and phase change problems with the eXtended finite element method. *Computational Mechanics*. accepted for publication.

[26] W.J. Rider and D.B. Kothe. Streaching and tearing interface tracking methods. In *AIAA Paper 95-1717 (LANL Report LA-UR-95-1145)*. presented at the 12th AIAA CFD Conference, San Diego CA (June 19-22, 1995).

[27] W.J. Rider and D.B. Kothe. Reconstructing volume tracking. *Journal of Computational Physics*, 141:112–152, 1998.

[28] J. A. Sethian. *Level set methods and fast marching methods*. Cambridge University Press, 1999.

[29] N. Sukumar, D. L. Chopp, N. Moës, and T. Belytschko. Modeling holes and inclusions by level sets in the extended finite element method. *Computer Methods in Applied Mechanics and Engineering*, 2000. Submitted.

[30] M. Sussman, A. Almgren, J. B. Bell, P. Colella, L. H. Howell, and M. L. Welcome. An adaptive level set approach for incompressible two-phase flows. *Computational Physics*, 148:81–124, 1999.

[31] M. Sussman and E. Fatemi. An efficient interface preserving level set re-distancing algorithm and its applications to interfacial incompressible fluid flow. *Journal of Scientific Computing*, 20(4):1165–1191, 1999.

[32] M. Sussman, E. Fatemi, P. Smereka, and S. Osher. An improved level set methos for incompressible two-phase flows. *Computers and Fluids*, 27(5):663–680, 1997.

[33] M. Sussman, P. Smereka, and S. Osher. A level set approach for computing solutions to incompressible two-phase flows. *Journal of Computational Physics*, 114:146–159, 1994.

[34] T.E. Tezduyar, M. Behr, and J. Liou. A new strategy for finite element flow computations involving moving boundaries and interfaces-the deforming-spatial-domain/space-time procedures: I. The concept and preliminary tests. *Computer Methods in Applied Mechanics and Engineering*, 1992.

[35] T.E. Tezduyar, M. Behr, S. Mittal, and J. Liou. A new strategy for finite element flow computations involving moving boundaries and interfaces-the deforming-spatial-domain/space-time procedures: II. Computation of free-surface flows, two-liquid flows and flows with drifting cylinders. *Computer Methods in Applied Mechanics and Engineering*, 1992.

[36] A.S. Usmani, J.T. Cross, and R.W. Lewis. A finite element model for he simulations of mould filling in metal casting and associated heat transfer. *International Journal of Numerical Methods in Engineering*, 35:787–806, 1992.

[37] G.J. Wagner, N. Moës, W.K. Liu, and T. Belytschko. The extended finite element method for rigid particles in Stokes flow. *International Journal for Numerical Methods in Engineering*, 51(3):293–313, 2001.

[38] O.C. Zienkiewicz and R. Codina. A general algorithm for compressible and incompressible flow, Part I. The split characteristic based scheme. *International Journal of Numerical Methods in Fluids*, 20:869–85, 1995.

[39] O.C. Zienkiewicz and R.L. Taylor. *The finite element method, Volume 3: Fluid dynamics*. Butterworth and Hienemann, 2000.